Applied Clay Science 162 (2018) 351–361

Contents lists available at ScienceDirect

Applied Clay Science

journal homepage: www.elsevier.com/locate/clay

Research paper

Quantitative and structural analysis of minerals in soil clay fractions developed under different climate zones in China by XRD with Rietveld method, and its implications for pedogenesis

Wei Zhao[a,b], Wen-Feng Tan[b,c,*]

[a] State Key Laboratory of Soil Erosion and Dryland Farming on the Loess Plateau, Northwest A&F University, Yangling, Shaanxi Province 712100, PR China
[b] State Key Laboratory of Soil Erosion and Dryland Farming on the Loess Plateau, Institute of Soil and Water Conservation, Chinese Academy of Sciences and the Ministry of Water Resources, Yangling, Shaanxi Province 712100, PR China
[c] College of Resources and Environment, Huazhong Agricultural University, Wuhan 430070, PR China

ARTICLE INFO

Keywords:
X-ray diffraction
Quantification
Clay minerals
Iron (hydr)oxides
Soil development

ABSTRACT

Mineral compositions and structures in soil clay fractions can reflect the pedogenesis and the pedoenvironments of the natural soils. However, the simultaneous quantification and structural analysis of all phases in soils by X-ray diffraction are difficult, mainly due to overlapping reflections. In this study, quantification and structural analysis of the mineral phases in clay fractions in five soils (Alliti-Udic Ferrosol, Claypani-Udic Argosol, and Hapli-Udic Argosol, Malan loess, and Paleosol), developed under different climate zones in China, were carried out by the Rietveld method. Before proceeding with these analyses for the natural soil clay fractions by the Rietveld method, this method was applied to a set of artificial soils of montmorillonite (including a 6.8% quartz impurity), kaolinite, goethite, hematite, and magnetite to evaluate the accuracy of the method. Moreover, in the Rietveld method, the structure phase models, background function, profile models, the initial values for the correction of preferred orientation, and sequence of operations in Rietveld refinement parameters were optimized to improve the accuracy of the method. The evaluation demonstrated the quantitative analysis by the Rietveld method can obtain relatively satisfied results. The absolute errors for the mineral contents below 5% were in the range of −0.49%–+0.63%, and those for the mineral contents above 10% were in the range of −6.32%–+5.00%. The absolute errors for the Al-substitutions in the goethite and hematite are −0.8 Al mol %–+3.2 Al mol% and −0.3 Al mol%–+3.3 Al mol%, respectively. Employing the above Rietveld method, the content of every mineral and Al-substituted iron (hydr)oxides (goethite and hematite) in the clay fractions in the five soils developed under different climate zones were obtained. In combined with the soil physicochemical properties, the order of pedogenic development of the five natural soils is Alliti-Udic Ferrosol > Claypani-Udic Argosol > Hapli-Udic Argosol and > Malan loess, respectively.

1. Introduction

The minerals are the skeleton of soil and frequently used as indicators of pedogenesis in soil (Cornell and Schwertmann, 2003). During the weathering process the pre-existing clay mineral species may transform into other clay mineral phases (Singer, 1980). The transformation of illite also produces vermiculite (Wilson, 1999). Detrital chlorite tends to disappear by weathering to vermiculite (Banfield and Murakami, 1998) or smectite (Arocena and Sanborn, 1999), and vermiculite in turn weathers to form kaolinite and iron oxides (Dere et al., 2016). Kaolinite originates from almost all primary minerals (Wilson, 2004).

Iron (hydr)oxides are ubiquitous throughout the soils and sediments as fine particles and often present as coatings on the surfaces of aluminosilicate or phyllosilicate crystals (Wiriyakitnateekul et al., 2007). Iron (hydr)oxides are also major constituents of mottles and concretions in soils. Iron (hydr)oxides in soils vary in terms of such parameters as mineral species, crystal size, structural order and isomorphous substitution (Wiriyakitnateekul et al., 2007). Variations in these properties may reflect soil parent minerals and the conditions of pH, redox potential, moisture, and temperature in the soil environment (Schwertmann and Taylor, 1989). The degree of weathering and formation of pedogenic iron oxides and hydroxides is expressed by the ratio of citrate-dithionite-bicarbonate-extractable iron (Fe_d) to total

* Corresponding author at: State Key Laboratory of Soil Erosion and Dryland Farming on the Loess Plateau, Institute of Soil and Water Conservation, Chinese Academy of Sciences and the Ministry of Water Resources, Yangling, Shaanxi Province 712100, PR China
E-mail address: wenfeng.tan@hotmail.com (W.-F. Tan).

https://doi.org/10.1016/j.clay.2018.05.019
Received 29 March 2018; Received in revised form 16 May 2018; Accepted 17 May 2018
Available online 28 June 2018
0169-1317/

amounts of iron (Fe_t). An increasing Fe_d/Fe_t ratio reflects the progressive weathering of Fe-bearing minerals with time (Arduino et al., 1986). Goethite and hematite are the most common iron (hydr)oxides. Goethite occurs in different types of soils under various climatic conditions, whereas hematite is restricted to soils in warmer, predominantly subtropical and tropical climates (Torrent et al., 1980; Schwertmann and Kämpf, 1985; Cornell and Schwertmann, 2003; Rapp and Hill, 2006). For isomorphous substitution of Al for Fe in goethite, it can influence the crystallite size of goethite (Fey and Dixon, 1981; Liu et al., 1994) and account for the inherent structural and thermodynamic stability of goethite (α-FeOOH). In addition, the degree of Al-substitution in goethite reflects the immediate environment of pedogenesis (Fitzpatrick and Schwertmann, 1982). Al-substitution in soil hematite (Fe_2O_3) is very common in tropical soils as is the association of Al-hematite with Al-goethite (Liu et al., 1994; Cornell and Schwertmann, 2003).

Considering the indication of mineral composition and structure in soil clay fractions for pedogenesis, its quantitative phase analysis will help to better understand soil development. In general, combinations of two or more methods such as selective dissolution, chemical, thermal, and spectroscopic analyses, and XRD must be used to accomplish quantitative soil mineralogic analysis (Weidler et al., 1998; Alves and Omotoso, 2009; Dias et al., 2013; Prandel et al., 2014). For this reason, the conventional approaches used for this purpose are often expensive and time-consuming. Furthermore, some quantitative methods have drawbacks that give rise to inaccurate results. For instance, Mössbauer spectroscopy may provide the relative proportion of both crystalline and amorphous Fe phases, although it poses considerable difficulties in the correct interpretation of the Mössbauer spectra arising from the effects of Al substitution in the structure and small particle sizes (Gold et al., 1979). Rock magnetic methods (Dekkers, 1997) may be used to identify ferrimagnetic magnetite (Fe_3O_4) and maghemite (γ-Fe_2O_3) with extraordinary sensitivity. However, this method is inapplicable to identify the ordinary iron (hydr)oxides in soils, i.e. goethite and hematite, because the contribution of imperfect antiferromagnetic minerals to the overall magnetic properties is usually insignificant compared to the signal of magnetite, even when the magnetite content is low. Diffuse reflectance spectroscopy involves low detection limits and little time and effort, but the identification of iron (hydr)oxide minerals such as magnetite in soils is very restricted except for goethite and hematite (Malengreau et al., 1996; Ji et al., 2001; Barrón and Torrent, 2013). Routine X-ray diffraction is greatly hindered by the small crystallite and low contents of Fe (hydr)oxides in soils because these iron (hydr)oxides often produce reflections that are broad and weak compared to those produced by the clay mineral matrix.

The application of the Rietveld method to XRD data is a potential alternative method for accurate and fast soil quantitative mineralogic analyses. The mineralogical composition of a ferralitic soil was quantified by the XRD Rietveld method (Weidler et al., 1998). Alves et al. (2007) applied the XRD Rietveld method to quantify the mineral components in the oxisol clay fraction after iron-removal. Recently, Prandel et al. (2014) have obtained the quantitative composition of the minerals in several ultisol samples through the Rietveld method. Though these studies employed Rietveld refinement of X-ray diffraction (XRD) pattern to obtain relatively reliable XRD quantitative results for the soil mineral compositions, they focused on the highly-weathered soils, which contain relative high content of well-crystallized iron (hydr)oxide minerals (45.1–123.2 g Fe /kg soil sample, well-crystallized iron (hydr)oxide minerals including goethite, hematite, and magnetite) (Weidler et al., 1998; Brinatti et al., 2010; Dias et al., 2013). For the weakly-weathered soils which contain low contents of iron (hydr)oxide minerals, the Rietveld method is seldom applied. In this study, an improved method of X-ray diffraction combined with Rietveld refinement was established, in which corundum was used as an internal standard to calibrate the 2θ offset and the refinement was performed in the range of Bragg angle (4–85°). The method can be employed to obtain simultaneously the absolute content of minerals and unit-cell parameters of iron (hydr)oxides in natural soil clay fractions with high- or low-content iron (hydr)oxide minerals. This application is helpful to interpret the pedogenesis and pedoenvironments of natural soils.

2. Materials and methods

2.1. Collection and treatment of the natural soils

The samples were collected from the top 20–80 cm of the soil profiles in Guiyang in Hunan province (N 25.8°, E 112.7°), Wuhan in Hubei province (N 30.5°, E 114.3°), and Tai'an in Shandong province (N 36.2°, E 117.1°), respectively. The soils are Alliti-Udic Ferrosol, Claypani-Udic Argosol, and Hapli-Udic Argosol according to Chinese Soil Taxonomy (Cooperative Research Group on Chinese Soil Taxonomy, 2001) or Alumic Acrisol, Eutric Planosol, and Haplic Luvisol according to WRB reference system (IUSS Working Group WRB, 2014) from Guiyang, Wuhan, and Tai'an, respectively. The samples of loess and paleosol were taken from a Malan loess (L_1) and the most developed S_{5-3} soil profile in Wugong in Shaanxi province (N 34.3°, E 108.1°), respectively. These five natural soils were designated GY, WH, SD, WGL, and WGS, respectively (see Table 1). The soils GY, WH, and SD developed on middle Pleistocene (Q2) red clay, Late Pleistocene (Q3) Xiashu loess, and gneiss parent materials, respectively. WGL and WGS developed on the constant earthy accumulation formed under arid and semi-arid conditions during the Quaternary Period (Liu, 1985). The three natural soils (GY, WH, and SD) were selected on the basis of the different climate zones the three soils located. For the other two natural soils, WGS and WGL, though they are located in the same climate zone, they experienced an interglacial period and a glacial period in the past, respectively (Huang et al., 2011; Huang et al., 2012). The differences in the hydrothermal characteristics of climate lead to many differences in the pedogenesis of the natural soils. And the differences in pedogenesis result in the difference in the contents and compositions of the minerals in the natural soil clay fractions. So, the high distinction in the contents and compositions of the minerals is suitable to better estimate the applicability of the Rietveld method to the analysis of minerals in natural soil clay fractions.

Table 1
Basic properties and chemical extraction of iron (hydr)oxides in the natural soils.

Designated name	Soil types	pH	OM[a] (g/kg)	Chemical extraction of iron (hydr)oxides			Fe_o/Fe_d	Fe_d/Fe_t	$(Fe_d–Fe_o)/Fe_t$
				Fe_o(g/kg)	Fe_d(g/kg)	Fe_t(g/kg)			
GY	Alliti-Udic Ferrosol	6.12	7.4	1.07	44.4	59.5	0.024	0.75	0.73
WH	Claypani-Udic Argosol	6.27	22.6	6.27	31.9	53.8	0.2	0.59	0.48
SD	Hapli-Udic Argosol	7.30	22.1	2.13	22.1	52.9	0.096	0.42	0.38
WGS	Paleosol	8.24	2.7	1.15	24.5	74.6	0.047	0.33	0.31
WGL	Malan loess	8.12	6.2	0.49	17.7	58.7	0.028	0.30	0.29

Fe_d = dithionite-citrate-bicarbonate-extractable iron; Fe_t = total iron.
[a] OM = organic matter; Fe_o = oxalate-soluble iron.

The natural soil samples (approximately 50 g) were pretreated for further analysis with an acetic acid solution buffered with sodium acetate at pH 5.0 to remove calcium carbonate and with 10% H_2O_2 to remove organic matter. After the final treatment with H_2O_2, the samples were heated at a low temperature for approximately an hour to destroy excess H_2O_2. The precipitate was then washed several times with distilled water to remove excess ions and promote dispersion of the clays. The clay fraction (< 2 μm) was separated by the settling of particles in settling columns in accordance with Stokes' law (Stokes, 1845).

2.2. Preparation of artificial soils

2.2.1. Clay minerals and iron (hydr)oxides preparation

Raw kaolinite and montmorillonite were purchased from the Maoming Kaolin Clay Company (Guangdong Province, China) and Sanding Limited Company (Zhejiang Province, China), respectively, and purified as described in the literature (Kunze and Dixon, 1986). The particle fraction (< 2 μm) was collected by sedimentation following Stokes' law and dried at 40 °C, ground to pass a 100-mesh sieve, and stored in a desiccator.

Goethite, hematite, and magnetite were synthesized in accordance with the procedures described by Schwertmann and Cornell (2000). The final products were centrifuged and washed with oxygen-free distilled water until the conductivity of the supernatant was < 6 μS/cm. The precipitated iron (hydr)oxides were dried at 40 °C, ground to pass a 100-mesh sieve, and stored in a desiccator.

The three types of synthesized iron (hydr)oxides and kaolinite were pure and characterized by X-ray diffraction. The minor amount of quartz (6.8%) was found in montmorillonite using Whole Pattern Fitting and Rietveld Refinement of X-ray diffraction pattern with Materials Data Inc. (MDI) Jade software.

2.2.2. Artificial soils of clay minerals and iron (hydr)oxides

To simulate soil main composition, mixtures of the minerals prepared, including montmorillonite, quartz, kaolinite, goethite, hematite, and magnetite, were homogenized, mixing them in various ratios in an agate mortar for 5 min with acetone until its evaporation (Table 2). Corundum was added to the mixtures for use as an internal standard. The resulting samples were designated M1, M2, M3, M4, and M5. The artificial soils are used in the present study to establish the initial parameters of mineral structures and the sequence of operations in Rietveld refinement parameters. Also, the artificial soils are used to the accurate estimation for the Rietveld method mentioned above.

2.3. Physicochemical properties of natural soils

The total organic matter content was determined by the dichromate oxidation method (Nelson and Sommers, 1982). The soil pH was measured at a soil to water mass ratio of 1:1 by using a pH meter equipped with a calibrated combined glass electrode.

The amount of oxalate-soluble iron (Fe_o) in the clay fraction was measured using Schwertmann's method (1964). The amount of DCB-extractable iron (Fe_d) was determined using the method of Mehra and Jackson (1960). The amount of total iron (Fe_t) was determined by X-ray fluorescence using a Metorex (Finland) XMET920 system with a 3–20 keV probe (109 Cd source).

The low-frequency magnetic susceptibility (χ_{LF}) and high-frequency magnetic susceptibility (χ_{HF}) of the artificial soils and the natural soil clay fractions was measured using a Bartington magnetic susceptibility meter with an MS2B dual-frequency sensor at a frequency of 470 and 4700 Hz, respectively. The frequency-dependent susceptibility (χ_{FD}) was calculated using the formula $\chi_{FD} = (\chi_{LF}-\chi_{HF})/\chi_{LF} \times 100\%$ (Liu et al., 1992b; Shu et al., 2001).

2.4. Mineral phase analysis for the natural and artificial soils by X-ray diffraction

2.4.1. Qualitative and semi-quantitative analysis for clay minerals in the natural soils

To identify the phyllosilicate minerals in the clay fractions of the natural soils X-ray diffraction (XRD) was performed after removing free Al- and Fe-oxides from the fractions by the DCB extraction method (Mehra and Jackson, 1960). For the XRD measurements, specimens of the clay samples were saturated with magnesium (Mg) or with potassium (K) and mounted as slurries on glass slides. The air-dried Mg saturated specimens were analyzed at 25 °C after glycerol solvation for 24 h (Mg-glycerol). The air-dried K-saturated specimens were X-rayed at 25 °C before and after heating at 300 °C and 550 °C for 2 h (K-25 °C, K-300 °C, K-550 °C). All XRD patterns were recorded by a Bruker D8 Advance X-ray diffractometer equipped with a LynxEye detector using Ni-filtered CuKα radiation (λ = 0.15418 nm) generated with 40 kV, accelerating potential and 40 mA tube current, from 3 to 28° (2θ) at a scanning speed of 1° (2θ) min^{-1} at a step size of 0.02°.

Identification of the clay minerals is mainly based on the comparison of the XRD patterns obtained under the different measurement conditions (Fig. 1). Montmorillonite (Viani et al., 2002) was identified by the presence of the 1.8 nm reflection in the Mg-glycerol specimen and the absence of this reflection in all K specimens. Kaolinite (Bish and Von Dreele, 1989) was identified by the presence of a reflection at 0.71 nm in the Mg-glycerol, K-25 °C, and K-300 °C specimen. Vermiculite (Hendricks and Jefferson, 1938) was identified when the 1.4 nm

Table 2
Result of the quantitative mineralogical analysis with the Rietveld method in the artificial soils (% by weight).[a]

Sample		Minerals							R-factor
		Mt	Kaol	Goe	Hem	Mag	Q	Cor	
M1	Known	64.3	16.3	0.4	3.6	0.8	4.7	10.0	
	Rietveld method	64.0 (4.2)	14.8 (1.3)	0.4 (0.1)	3.7 (0.4)	1.3 (0.5)	4.3 (0.3)	11.5 (0.3)	0.053
M2	Known	57.7	22.8	1.0	3.1	1.0	4.2	10.0	
	Rietveld method	56.0 (3.7)	24.6 (1.5)	1.3 (0.3)	2.5 (0.4)	1.3 (0.5)	4.3 (0.2)	10.0 (0.3)	0.056
M3	Known	52.6	28.4	0.9	2.5	1.4	3.8	10.4	
	Rietveld method	47.6 (3.1)	31.8 (1.4)	0.7 (0.2)	2.4 (0.5)	1.8 (0.5)	3.7 (0.2)	12.0 (0.3)	0.058
M4	Known	39.7	41.4	2.0	1.9	2.3	2.9	10.0	
	Rietveld method	36.8 (2.7)	42.7 (1.8)	2.4 (0.3)	1.6 (0.4)	2.3 (0.6)	2.7 (0.2)	11.5 (0.3)	0.060
M5	Known	29.5	53.1	2.0	0.6	3.1	2.2	9.6	
	Rietveld method	26.9 (2.3)	57.2 (2.2)	1.8 (0.3)	0.8 (0.2)	2.9 (0.7)	2.0 (0.3)	8.6 (0.4)	0.071

[a] Samples M1, M2, M3, M4, and M5 are the artificial soils. Corundum was added to the artificial soils and used as an internal standard. Letters indicate: Mt., montmorillonite; Kaol, kaolinite; Goe, goethite; Hem, hematite; Mag, magnetite; Q, quartz (the impurity in montmorillonite); Cor, corundum. The value of R-factor indicates the quality of fit. The value in the parentheses is the error of fitting.

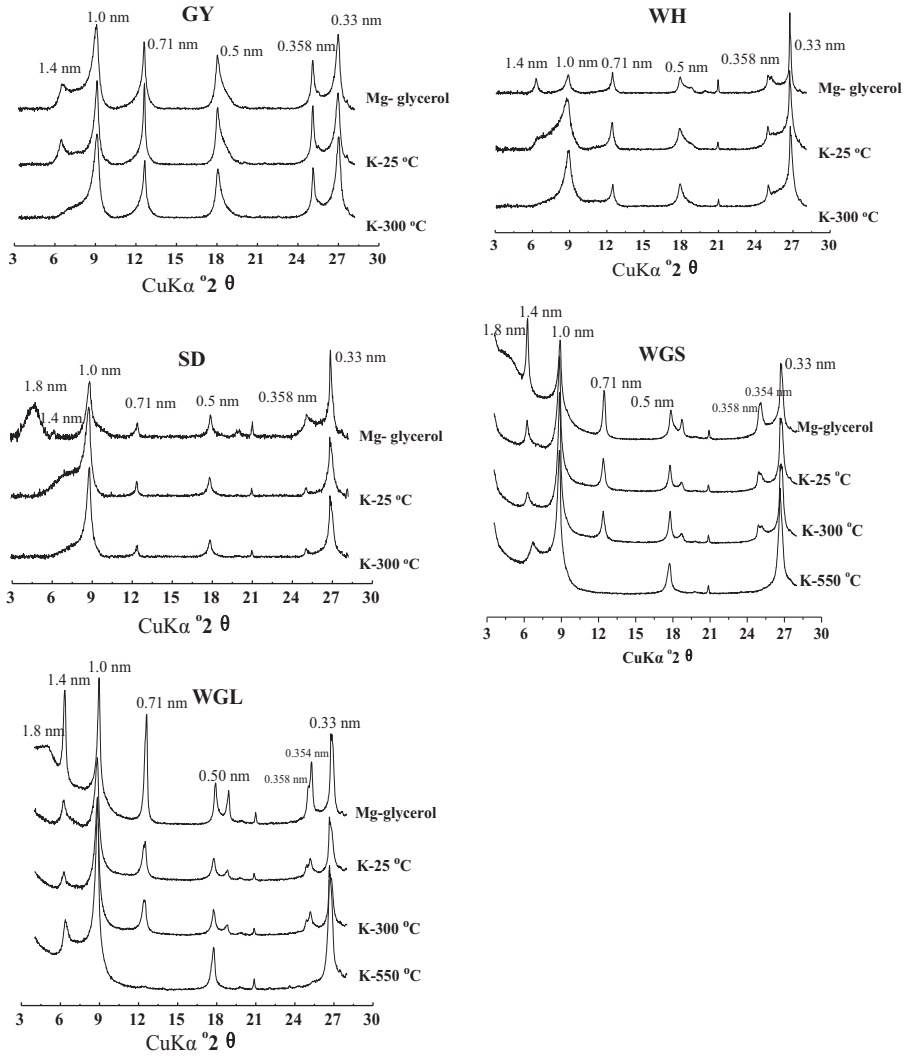

Fig. 1. XRD patterns (CuKα) with Mg-glycerol salvation and K-treatments of oriented clay samples of the natural soils.

reflection in the K-25 °C specimen was absent compared to that in the Mg-glycerol specimen. Illite (Drits et al., 2010) was recognized by its 1.0 nm reflection in all treatments. Chlorite (Lister and Bailey, 1967) maintained a 1.4 nm reflection after heat treatment of 2 h at K-550 °C.

Semi-quantitative estimates of the proportions of the clay minerals in the clay fractions were derived from the integrated areas of the characteristic reflections (Pai et al., 1999). The relative mass percentages of clay minerals were determined using empirically estimated weighting factors (Xiong, 1985). Kaolinite and chlorite were identified by the presence of a reflection at 0.71 nm and separated by the reflections at 0.358 nm (kaolinite) and 0.354 nm (chlorite) in the Mg-glycerol specimen.

2.4.2. Quantitative and structural analysis for minerals in natural and artificial soils by the Rietveld method

The Rietveld method, as was indicated, fits point-to-point the experimental intensities of the whole pattern to those calculated. The "Whole Pattern Fitting" refinement mode included in MDI Jade 6.0 software, was used in the present work and allows the refinement and subsequent quantitative analysis to be made.

The natural soil clay fractions and artificial soils were ground to a particle size of smaller than 10 μm to reduce the micro-absorption. The sample was back-filled into an Al holder with a hole to minimize the effects of preferred orientation of particles when the sample is filled from the top of the cavity and smoothed with a glass slide. Powder XRD patterns (CuKα radiation, λ = 0.15418 nm, 40 kV and 40 mA, divergence slit of 0.2 mm, antiscatter slit of 4°, discrimination lower level of 0.18) were collected using a Bruker D8 Advance (Bruker, Germany) powder diffractometer with a LynxEye detector. Here the discrimination lower level is set as 0.18 to minimize the effect of the fluorescence of Fe from iron (hydr)oxides by Cu radiation on background and reflection intensities in XRD analyses. The intensities were measured at 0.02°2θ intervals, with a 1.2-s counting time per step over the range of 4°to 85°2θ.

The refinements were performed over a range of 4–85°2θ. Fig. 2 shows a flowchart of the Rietveld refinement procedure. The instrumental FWHM curve, i.e. instrumental broadening, was estimated using a reference Si powder (Standard Reference Material 640b of NIST). The profile parameter (f0, f1, and f2) for all phases was initialized based on the obtained instrumental FWHM curve. The estimated standard deviations of f1 and f2 parameters will be large due to the severe overlapping of reflections of multiple phases with each other. So f1 and f2 were not refined, and their values were fixed to zero. The option of refinement controls, Damp Parameter Shifts, was selected to limit the maximum shifts allowed per iteration for different refinable parameters. This restriction can help refinement convergence in a multiphase refinement in which interdependency among refinable parameters is high due to severe overlapping of reflections. Before Rietveld refinement, the choice of structure phase models, background function, profile models, the correction of preferred orientation, and sequence of

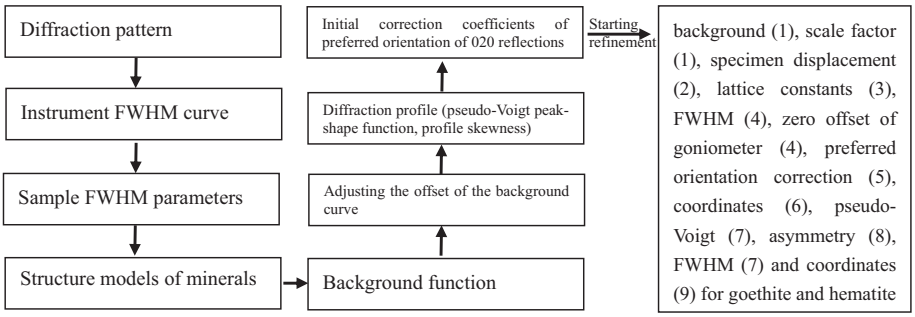

Fig. 2. Flowchart of the Rietveld refinement procedure. The number in parentheses indicates the round of assignment.

Table 3
Initial correction coefficient of preferred orientation of 020 reflection for clay minerals in Rietveld method.

Height of Kα1 reflection (CPS)							Correction coefficient of preferred orientation of 020 reflection[a]				
Sample	Reflection at 1.4 nm	Reflection at 1.0 nm	Reflection at 0.72 nm	Height ratio of reflection at ~1.4 nm to reflection at ~0.72 nm	Height ratio of reflection at ~1.0 nm to reflection at ~0.72 nm	Mt	Kaol	I	Verm	Chl	offset
M1	10,968(47)[b]	–	1255(36)	8.83	–	0.5	4.42	–	–	–	0.3
M2	10,016(42)	–	1829(38)	5.47	–	0.5	2.74	–	–	–	0.33
M3	10,884(53)	–	2624(54)	4.14	–	0.5	2.07	–	–	–	0.49
M4	6602(36)	–	3793(51)	1.74	–	1	1.74	–	–	–	0.63
M5	5547(32)	–	5345(52)	1.04	–	1	1.04	–	–	–	0.45
GY	123(12)	335(10)	371(14)	0.33	0.9	–	1.9	1	0.33	–	0.45
WH	520(18)	165(18)	282(13)	1.84	0.59	–	2.43	1	1	–	0.6
SD	792(16)	145(11)	101(9)	7.84	1.44	0.5	4.64	0.5	0.5	–	0.44
WGL	400(17)	445(19)	384(14)	1.04	1.16	1	3.51	1	0.35	0.35	0.43
WGS	288(20)	488(19)	274(14)	1.05	1.78	1	4.13	1	0.35	0.35	0.43

[a] Mt. = montmorillonite; Kaol = kaolinite; I = illite; Chl = chlorite; Verm = vermiculite.
[b] The value in the parentheses is the error of fitting.

operations in Rietveld refinement parameters is important for an accurate result. The starting crystallographic data used for each phase model were extracted from the literature (described in more detail later). The amorphous background mode was selected as the background function. The tie points in the background were sampled automatically by successive applications of pattern smoothing - causing sharp reflections to be truncated. The offset of the background curve from background points was adjusted to make the background of the observed corundum reflections within the range of 2theta 60°-85° just over the background curve, and the offset values are listed in Table 3. The offset of the background curve was determined based on the background at a high diffraction angle due to its little disturbance from X-ray fluorescence. The diffraction profile was modeled by a pseudo-Voigt peak-shape function (PSF). The pseudo-Voigt PSF can also be tailored into a Gaussion or Lorentzian PSF by the mixing/Lorentzian factor (p0). The mixing/Lorentzian factor was initially set as 0.5 and refined. The profile skewness can be adjusted by the profile asymmetry factor (s0). The profile asymmetry factor was initially set as 0.5 and refined. For the preferred orientation of clay minerals, 020 reflections of clay minerals were selected to correct because 020 reflection is the characteristic reflections for the different clay minerals and the 020 reflections overlap greatly. By the pre-refinement, we found the initial correction coefficients of preferred orientation of 020 reflections for clay minerals can be obtained on the basis of the Kα1 reflection heights at ~1.4, ~1.0, and ~0.72 nm of clay minerals in the section 2.4.3. The Kα1 reflection heights at ~1.4, ~1.0, and ~0.72 nm of clay minerals with the profile fitting method in the range of 2theta 4-14° were implemented in MDI Jade software. During the refinement, to make the contribution of weak reflections to the residual R-factor the same as that of the strong reflections and to emphasize the high-angle reflections in lattice constant refinement, the overall weighting of a scanning data point (i) was used and defined as a function of the 2-theta angle and the intensity of the XRD reflection, i.e. wt(i) = Sin(theta)/I(i). Finally, the round of refinement for each parameter was assigned: background (1), scale factor (1), specimen displacement (2), lattice constants (3), FWHM (4), zero offset of goniometer (4), preferred orientation correction (5), coordinates (6), pseudo-Voigt (7), asymmetry (8), where the number in parentheses indicates the round of assignment. To avoid the influence of reflections of clay minerals on the reflections of goethite and hematite during the Rietveld refinement, the round of FWHM and coordinates for the two iron (hydr)oxides were assigned to 7 and 9, respectively.

The initial structural models of clay minerals were taken from the XRD data of (Lister and Bailey, 1967) for chlorite, (Drits et al., 2010) for illite, (Bish and Von Dreele, 1989) for kaolinite, (Hendricks and Jefferson, 1938) for vermiculite, and (Viani et al., 2002) for montmorillonite. The initial structural models of goethite, hematite, and magnetite in the soils, which were designated Goe, Hem, and Mag, were taken from the XRD data of Hazemann et al. (1991), Blake et al. (1966), and O'Neill and Dollase (1994), respectively. In addition, the initial structural models of corundum, quartz, and gibbsite were taken from the XRD data of Lutterotti and Scardi (1990), Antao et al. (2008), and Balan et al. (2006), respectively. The A1-substitution in goethite was determined from the unit cell dimension *c* in units of Å (obtained from the Rietveld refinement) using the equation A1 (mole %) = 1730–572 *c* (Schulze, 1984). The A1-substitution in hematite was estimated from the *a* dimension in units of Å (obtained from the Rietveld refinement) using the equation A1 (mole %) = 3109–617.1 *a* (Schwertmann et al., 1979).

2.4.3. Initial correction coefficients of preferred orientation of 020 reflections for clay minerals

If only montmorillonite and kaolinite are present in samples, the

initial correction coefficients of preferred orientation of 020 reflections for montmorillonite and kaolinite are obtained on the basis of the ratio of the fitting values of 00 l Kα1 reflection heights of the two minerals (Eq. 1):

$$R_1 = (H_1/H_2)/m_0 \quad (1)$$

Where R_1 is the ratio of the fitting values of 00 l Kα1 reflection heights of montmorillonite and kaolinite, H_1 the fitting value of 001 Kα1 reflection height of montmorillonite, and H_2 the fitting value of 001 Kα1 reflection height of kaolinite, m_0 is a constant and set as 1.

The initial correction coefficient of preferred orientation of 020 reflection for kaolinite is set as the value of H_1/H_2, the corresponding initial correction coefficient for montmorillonite is set as m_0. If $H_1/H_2 > 2$, by pre-analysis, the initial correction coefficient of preferred orientation of 020 reflection for kaolinite is set as the value of $0.5*(H_1/H_2)$ better, and the corresponding initial correction coefficient for montmorillonite is set as $0.5*m_0$. In this case, good results can be obtained.

If more types of clay minerals are present in samples, the initial correction coefficients of preferred orientation of 020 reflections for clay minerals can be obtained as follows:

The initial correction coefficients of preferred orientation of 020 reflections for clay minerals (montmorillonite, kaolinite, chlorite, and vermiculite) are obtained by pre-analysis on the basis of the fitting values of Kα1 reflection heights at ~1.4 nm and ~0.72 nm of diffraction pattern (Eq. 2):

$$R_2 = ((H_3/n)/H_4)/m_1 \quad (2)$$

Where R_2 is the ratio of the fitting values of 00 l Kα1 reflection heights of 1.4 nm minerals (montmorillonite, chlorite, and vermiculite) to that of the Kα1 reflection height of ~0.72 nm, H_3 the fitting value of Kα1 reflection height at ~1.4 nm, H_4 the fitting value of Kα1 reflection height at ~0.72 nm, n the number of species of 1.4 nm minerals included in the sample, and m_1 is a constant and set as 1.

For montmorillonite, the initial correction coefficient for montmorillonite is set as m_1, the corresponding initial part correction coefficient (p_1) of preferred orientation of 020 reflection for kaolinite is set as the value of $(H_3/n)/H_4$. If $(H_3/n)/H_4 > 2$, the initial part correction coefficient of preferred orientation of 020 reflection for kaolinite is set as the value of $0.5*(H_3/n)/H_4$, and the corresponding initial correction coefficient for montmorillonite is set as $0.5*m_1$.

For chlorite or vermiculite, If $(H_3/n)/H_4 > 1$, the initial correction coefficient for chlorite or vermiculite is set as m_1, the corresponding initial part correction coefficient (p_2 or p_3) of preferred orientation of 020 reflection for kaolinite is set as the value of $(H_3/n)/H_4$; If $(H_3/n)/H_4 > 2$, the initial part correction coefficient of preferred orientation of 020 reflection for kaolinite is set as the value of $0.5*(H_3/n)/H_4$, and the corresponding initial correction coefficient for chlorite or vermiculite is set as $0.5*m_1$; If $(H_3/n)/H_4 < 1$, the initial part correction coefficient (p_2 or p_3) of preferred orientation of 020 reflection for kaolinite is set as the value of m_1, the corresponding initial correction coefficient for chlorite or vermiculite is set as $(H_3/n)/H_4$.

The initial correction coefficient of preferred orientation of 020 reflection for illite is obtained by pre-analysis on the basis of the fitting values of Kα1 reflection heights at ~1.0 nm and ~0.72 nm of the diffraction pattern (Eq. 3):

$$R_3 = (H_5/H_4)/m_1 \quad (3)$$

Where R_3 is the ratio of the fitting value of 001 Kα1 reflection height of illite to that of the Kα1 reflection height of ~0.72 nm, H_5 the fitting value of 001 Kα1 reflection height of illite, H_4 the fitting value of Kα1 reflection height at ~0.72 nm, and m_1 is a constant and set as 1.

For illite, the initial correction coefficient for illite is set as m_1, the corresponding initial part correction coefficient (p_4) of preferred orientation of 020 reflection for kaolinite is set as the value of H_5/H_4; If $H_5/H_4 > 2$, the initial part correction coefficient of preferred orientation of 020 reflection for kaolinite is set as the value of $0.5*H_5/H_4$, and the corresponding initial correction coefficient for illite is set as $0.5*m_1$.

Therefore, the initial total correction coefficient of preferred orientation of 020 reflection for kaolinite is the sum of the initial part correction coefficient (p_1, p_2, p_3, and p_4) mentioned above for kaolinite,

$$p_t = p_1 + p_2 + p_3 + p_4 \quad (4)$$

where p_t is the initial total correction coefficient of preferred orientation of 020 reflection for kaolinite.

3. Results and discussion

3.1. Chemical extraction of iron (hydr)oxides in the natural soils

Total iron, DCB-extractable iron, and oxalate-extractable iron (Fe_t, Fe_d, and Fe_o) in the natural soil clay fractions are presented in Table 1. The Fe_o content ranges from 0.49 to 6.27 g/kg. The Fe_d content ranges from 17.7 to 44.4 g/kg.

The Fe_d/Fe_t and $(Fe_d–Fe_o)/Fe_t$ ratios may be used as a geochemical index for pedogenesis. The Fe_d/Fe_t ratio ranges from 0.30 to 0.75, and the $(Fe_d–Fe_o)/Fe_t$ ratio ranges from 0.29 to 0.73, which show that the pedogenesis of GY is highest and that of SD is lowest among the soils GY, WH, and SD, and that the pedogenesis of WGS is stronger than that of WGL due to an increase of Fe_d with progressive weathering of Fe-bearing minerals (Torrent et al., 1980; Guo et al., 2000; Cornell and Schwertmann, 2003; Torrent et al., 2010). Because the Fe_o content may reflect the amount of ferrihydrite (Schwertmann, 1964), the Fe_o/Fe_d ratio between 0.024 and 0.2 indicates a small amount of ferrihydrite in the five natural soils.

3.2. Magnetic characterization of the artificial and natural soils

The values of χ_{LF}, χ_{HF}, and χ_{FD} of the artificial soils and natural soil clay fractions are listed in Table 4. The χ_{LF} reflects the amount of ferrimagnetic material and a high correlation between the χ_{LF} and the relative amount of magnetite ($\chi_{LF} = 451.6 \times$ magnetite% - 34.5; $R^2 = 0.9954$; $n = 5$, $P < 0.001$) in the artificial soils was found. The χ_{LF} of the clay fractions of natural soils GY, WH, and SD is very low ($11.1–45.5 \times 10^{-8}$ m^3/kg), which indicates that there is little ferrimagnetic material, such as magnetite. The χ_{LF} of the clay fractions of natural soils WGS and WGL, however, is very high (234.8×10^{-8} m^3/kg and 169.4×10^{-8} m^3/kg, respectively), which suggests that ferrimagnetic materials are present.

Because χ_{FD} is a proxy for the relative abundance of ultrafine (< 10 nm) superparamagnetic particles (Geiss et al., 2004), the values of χ_{FD} ranging from 1.1% to 1.8% (< 5%) in the artificial soils suggest that there are few ultrafine superparamagnetic grains (Fine et al., 1992; 1993). This result is consistent with the average crystallite size obtained by fitting the entire XRD pattern of goethite, hematite, and magnetite prepared in this study (32.5 ± 1.4 nm for goethite, 32.5 ± 0.4 nm for hematite, and 28.4 ± 0.3 nm for magnetite, respectively). The χ_{FD} of

Table 4
Magnetic properties of the artificial and natural soils.

Sample	χ_{LF} (10^{-8} m^3/kg)	χ_{HF} (10^{-8} m^3/kg)	χ_{FD} (%)
M1	294.3	291.1	1.1
M2	470.2	462.1	1.7
M3	624.7	616.5	1.3
M4	985.3	969.1	1.7
M5	1358.8	1334.3	1.8
GY	45.5	39.0	14.2
WH	14.7	12.8	12.5
SD	11.1	10.4	5.9
WGS	234.8	206.3	12.1
WGL	169.4	151.7	10.4

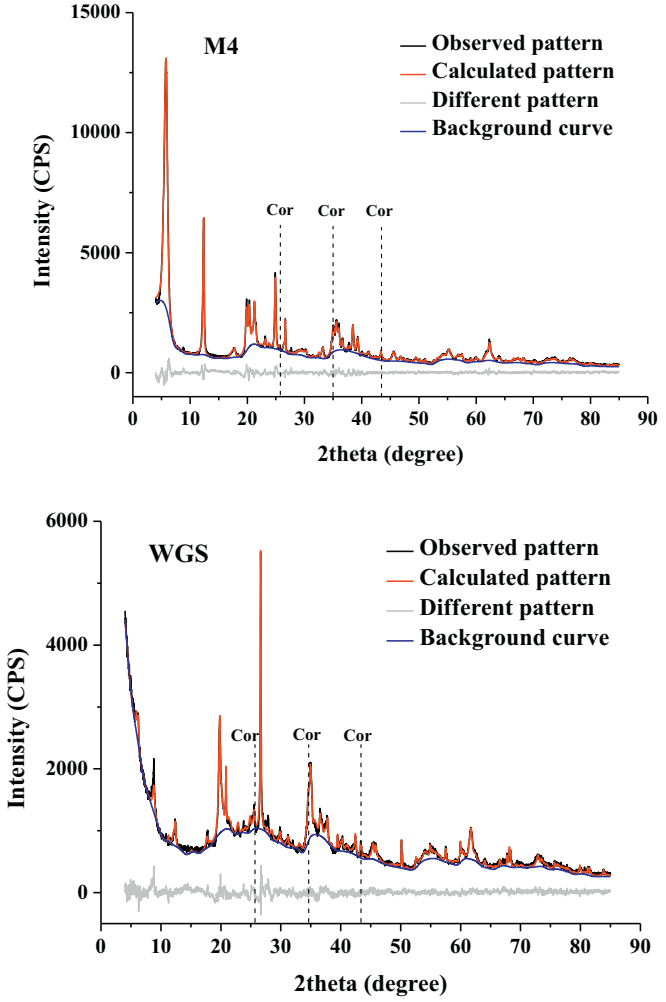

Fig. 3. Observed and calculated XRD patterns for the artificial soil (M4) and the natural soil (WGS). Cor indicates the reflections of corundum.

the natural soil clay fractions ranges from 5.9% to 14.2% (> 5%), and the order of the χ_{FD} values in these soil clay fractions is GY > WH > SD and WGS > WGL, respectively. This order suggests that the number of superparamagnetic grains is greatest in GY and lowest in SD and that the number of superparamagnetic grains in WGS is larger than that in WGL. Assuming that the ultrafine superparamagnetic grains originated primarily from pedogenesis (Liu et al., 1992a; Hao and Guo, 2001), the order of the pedogenesis of the natural soils is GY > WH > SD, and WGS > WGL, respectively.

3.3. Analysis of mineral phases in the artificial soils

The initial correction coefficients of preferred orientation of 020 reflections for montmorillonite and kaolinite are listed in Table 3. Fig. 3 shows the calculated pattern generated by the Rietveld method agrees with the experimental pattern (M4 sample as an example). The absolute errors between the calculated values and the known values of mineral contents below 5% were in the range of −0.49%–+0.63%. The absolute errors between the calculated values and the known values of mineral contents above 10% were in the range of −6.32%–+5.00%. Moreover, the dots in the scatter plots of Known vs Rietveld values lie closely to a straight line that the slope is 1 (Fig. 4). Al-substitutions in

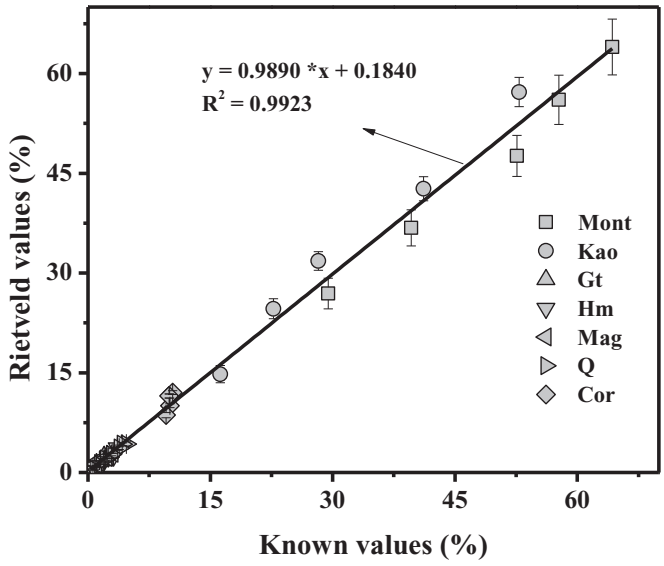

Fig. 4. Relation between the known and Rietveld values for the artificial soils. Mt. = montmorillonite; Kaol = kaolinite; Mag = magnetite; Goe = goethite; Hem = hematite; Cor = corundum; Q = quartz. Error bars represent estimated standard deviation of least-squares fits.

the goethite and the hematite, which were calculated from the cell parameters (−0.8 Al mol%–+3.2 Al mol% for goethite and −0.3 Al mol%–+3.3 Al mol% for hematite), are close to the known values (Al-substitution is zero for both goethite and hematite), except for that of goethite (6.9 Al mol%) for M3 and hematite (−6.2 Al mol%) for M5 (Table 5). The method of analysis used in this study, therefore, can be considered a reliable method for estimating the absolute amounts of minerals and Al-substitution in iron (hydr)oxides in natural soil clay fractions.

3.4. Clay minerals in the natural soils

The semi-quantitative phyllosilicate compositions of the natural soils by the oriented aggregate XRD technique (Hardy and Tucker, 1988) are summarized in Table 6. On the other hand, the absolute contents of clay minerals were generated by the Rietveld refinement and listed in Table 6. Fig. 3 shows the calculated pattern generated by the Rietveld method agrees with the experimental pattern (WGS sample as an example). To facilitate the comparison between the Rietveld results and those obtained from the oriented aggregate XRD technique, the clay mineral mass percentages determined by the Rietveld method were recalculated for each sample to a total of 100% (i.e. according to the montmorillonite + vermiculite + chlorite + illite + kaolinite = 100% formula). Fig. 5 shows the relation between the recalculated proportion of each clay mineral in each natural soil clay fraction and the mass percentage of the same clay mineral from the oriented aggregate study. And the dots in the scatter plots of relative contents by the semi-quantitative method vs by the Rietveld method lie closely to a straight line that the slope is 1, indicating that the relative contents of clay minerals by the Rietveld method agree with those by the semi-quantitative method.

3.5. Iron (hydr)oxides in the natural soil clay fractions

Iron (hydr)oxides in the natural soil clay fractions were quantified by the Rietveld method mentioned above. The type of Iron (hydr)oxides included in the whole-pattern fitting of the XRD patterns based on the

Table 5
Cell parameters and Al-substitution for goethite and hematite for the artificial and the natural soils[a].

Sample	Goe				Hem		
	Unit-cell edge lengths/Å			Al/mol %	Unit-cell edge lengths/Å		Al/mol %
	a	b	c		a	c	
M1	4.6017	9.9498	3.0227	1.0	5.0386	13.7549	−0.3
M2	4.5754	9.9490	3.0258	−0.8	5.0381	13.7764	0
M3	4.6254	9.9273	3.0124	6.9	5.0328	13.7736	3.3
M4	4.6120	9.9394	3.0199	2.6	5.0374	13.7808	0.4
M5	4.6141	9.9484	3.0189	3.2	5.0482	13.7581	−6.2
GY	4.6006	9.9344	2.9802	25.3	5.0387	13.8023	0[b]
WH	4.5921	9.9529	2.9957	16.5	5.0447	13.8309	0
SD	4.5947	9.9298	3.006	10.6	5.0452	13.8646	0
WGL	4.5968	9.9877	3.0106	7.9	5.0581	13.8202	0
WGS	4.5935	9.9261	3.0063	10. 4	5.0410	13.8153	0

[a] Samples M1, M2, M3, M4, and M5 are the artificial soils. Letters indicate: Goe, goethite; Hem, hematite.
[b] The calculated values of Al mol% for hematite are negative (−12.4–−1.8) for the natural soil clay fractions and there is no physical significance. In this case, Al mol% for hematite is considered as zero.

Rietveld method was determined based on two considerations. To start with, goethite and hematite are likely present in the five natural soils (Schwertmann et al., 1982; Mizota and Longstaffe, 1996; Cornell and Schwertmann, 2003; Rapp and Hill, 2006). In addition, following the results of soil magnetic properties above, ferrimagnetic materials hardly occur in soil samples GY, WH, and SD, and certain amounts of ferrimagnetic materials occur in soil samples WGS and WGL. The ferrimagnetic material is considered to be magnetite to simplify the analysis because magnetite and maghemite are common ferrimagnetic materials in soils and distinguished difficultly between them using XRD due to their similar structure. Therefore, goethite and hematite were included in the whole-pattern fitting of the XRD patterns for soils GY, WH, and SD, and goethite, hematite, and magnetite for soils WGL and WGS.

The resulting absolute amounts of the iron (hydr)oxides in the clay fractions in the five natural soils were 2.3%–5.9% for goethite, 1.1%–3.3% for hematite, and 1.7%–2.6% for magnetite (Table 6). So the calculated contents of well-crystallized iron (hydr)oxides ranged from 28.5–60.2 g/kg, which are closed to the values by the chemical extraction (17.2–43.3 g/kg). The degrees of Al-substitution in the goethite and the hematite in the clay fractions in the five natural soils are 7.9 Al mol%–25.3 Al mol% and 0 Al mol%, respectively, which were calculated from unit cell of iron (hydr)oxides based on the empirical equations (Schwertmann et al., 1979; Schulze, 1984).

3.6. Implications of the minerals in the natural soil clay fractions for pedogenesis

The relative content of the kaolinite in order is GY > WH > SD (Table 6) indicating that the pedogenesis of GY is strong and the pedogenesis of SD is weak since kaolinite relative content is often interpreted as chemical weathering proxy (Gylesjö and Arnold, 2006). In addition, the presence of gibbsite in GY sample, accounting for 21.6% of the total minerals, indicates the GY soil is highly developed. The major components of WGS and WGL are illite, chlorite, vermiculite, kaolinite, and montmorillonite. The relative content of chlorite and vermiculite in WGS is the two third of and closed to that in WGL, respectively. The soils WGS and WGL have nearly constant and low quantities of kaolinite. The relative content of illite in WGS is higher than that in WGL, implying that the pedogenesis of WGS is stronger than that of WGL since the relative content of illite increases with pedogenesis (Gylesjö and Arnold, 2006).

As shown in Table 6, the order of the Hem/(Goe + Hem) ratio in the natural soil clay fractions is GY (0.36) > WH (0.26) > SD (0.25) and WGS (0.41) > WGL (0.30), respectively, which is consistent with the orders of pedogenesis of the five natural soils based on the χ_{FD} values and Fe_d/Fe_t and $(Fe_d–Fe_o)/Fe_t$ ratios. Using the Hem/(Goe + Hem) ratio as a sensitivity proxy aids in the interpretation of the pedogenesis. In the soils GY, WH, and SD in succession from south to north, the relative amount of goethite increases and that of hematite decreases with the decrease in pedogenesis. In the soils WGS and WGL, the relative amount of goethite increases and that of hematite decreases with the decrease in the pedogenesis. This change in mineralogy is associated with variations in the climate, from relatively warm and wet in southern China to relatively cold and dry in northern China for GY, WH, and SD, and from typical of an interglacial period to typical of a glacial period for WGS and WGL. The goethite, therefore, indicates cold and dry conditions, while the hematite indicates warm and wet conditions, which is similar to the conclusions reported by Ji et al. (2001).

In addition, the amount of magnetite is lower and the amount of hematite is higher in the paleosol (WGS) than in the loess (WGL) (Table 6). This result is attributed to the transformation of primary magnetite to superparamagnetic maghemite or hematite, based on their similar parent minerals (Lagoeiro, 1998). The magnetic susceptibility and frequency-dependent susceptibility of WGS, thus, are higher than those of WGL (Table 4).

Table 5 shows that the goethite contains more Al in its structure than does the hematite, which is attributed to Al going preferentially into goethite (Cornell and Schwertmann, 2003). The amount of Al-substitution in the goethite and hematite may reflect the pedogenesis and the pedoenvironments of the natural soils. And highly Al-substituted goethite characterizes a pedogenic environment of strong desilication (Fontes and Weed, 1991). In this paper, the degree of Al-substitution in the goethite in the soils GY, WH, and SD decrease from south to north, which confirms the conclusion that the pedogenesis of GY is higher than that of WH and SD. The degree of Al-substitution in the goethite is higher in WGS than that in WGL, which confirms that the pedogenesis of WGS is higher than that of WGL.

4. Conclusions

Rietveld refinement served as a reliable method for quantifying the absolute amounts and analyzing the structures of minerals in natural soil clay fractions was established on a set of artificial soils of montmorillonite (including a 6.8% quartz impurity), kaolinite, goethite,

Table 6
Mineral compositions of the natural soil clay fractions.

Phase	Mineral content (% by weight)														
	Oriented aggregate XRD technique[b] (relative content)					Rietveld method									
						Relative content[c]					Absolute content				
	GY	WH	SD	WGL	WGS	GY	WH	SD	WGL	WGS	GY	WH	SD	WGL	WGS
Mt[a]	0	0	21.3	3.9	2.7	–	–	23.0 (3.6)	4.2 (1.2)	3.0 (1.0)	–	–	17.4 (2.7)	2.5 (0.7)	2.0 (0.7)
Kaol	28.9	21.7	4.6	8.8	6.4	25.3 (3.7)	22.7 (2.8)	6.5 (1.3)	6.1 (1.3)	5.4 (1.8)	14.5 (2.1)	14.7 (1.8)	4.9 (1.0)	3.7 (0.8)	3.6 (1.2)
I	62.5	60.1	72.6	66.1	70.0	69.1 (4.4)	62.9 (3.2)	64.3 (6.3)	69.0 (4.6)	73.1 (7.9)	39.7 (2.5)	40.8 (2.1)	48.7 (4.8)	41.8 (2.8)	49.3 (5.3)
Chl	–	–	–	15.7	6.8	–	–	–	12.8 (2.0)	8.4 (2.2)	–	–	–	7.7 (1.2)	5.6 (1.5)
Verm	8.6	18.2	1.5	5.4	14.1	5.6 (1.2)	14.5 (2.0)	6.2 (0.9)	8.0 (1.5)	10.2 (2.5)	3.2 (0.7)	9.4 (1.3)	4.7 (0.7)	4.9 (0.9)	6.9 (1.7)
Mag											–	–	–	2.6 (0.7)	1.7 (0.8)
Goe											5.9 (0.7)	3.5 (0.4)	3.3 (1.0)	2.6 (0.7)	2.3 (1.0)
Hem											3.3 (0.3)	1.2 (0.3)	1.1 (0.5)	1.1 (0.4)	1.6 (0.5)
Cor											11.9 (0.7)	11.6 (0.5)	8.3 (0.7)	15.3 (0.8)	8.9 (1.2)
Q											–	18.7 (0.6)	11.7 (0.8)	17.9 (0.8)	18.0 (1.4)
Gib											21.6 (2.0)	–	–	–	–
Hem/(Goe + Hem)											0.36	0.26	0.25	0.3	0.41

– = not detectable.

[a] Mt. = montmorillonite; Kaol = kaolinite; I = illite; Chl = chlorite; Verm = vermiculite; Mag = Magnetite; Goe = Goethite; Hem = Hematite; Cor = corundum; Q = quartz (the impurity in montmorillonite); Gib = gibbsite.

[b] Oriented aggregate XRD technique is semi-quantitative for clay mineral compositions of the natural soils.

[c] Absolute content indicates that the mass percentage of one type of soil mineral accounting for the total of soil minerals, which is obtained directly from Rietveld refinement, and the relative content indicates that the mass percentage of one type of clay mineral accounting for the total of clay minerals (i.e. montmorillonite + vermiculite + chlorite + illite + kaolinite = 100%). The value in the parentheses is the error of fitting.

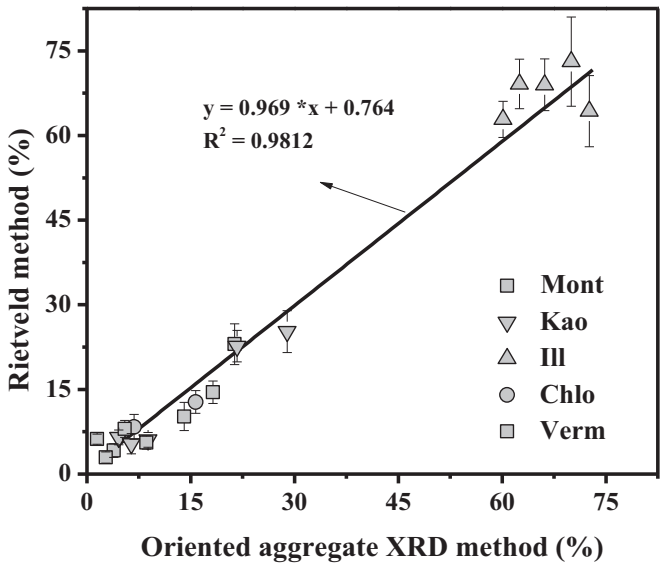

Fig. 5. Relation between the relative contents of minerals in the natural soil clay fractions by the oriented aggregate XRD technique (i.e. the semi-quantitative method) and by Rietveld method. Mt. = montmorillonite; Kaol = kaolinite; I = illite; Chl = chlorite; Verm = vermiculite. Error bars represent estimated standard deviation of least-squares fits. To facilitate the comparison between the Rietveld results and those obtained from the oriented aggregate XRD technique, the clay mineral mass percentages determined by the Rietveld method were re-calculated for each sample to a total of 100% (i.e. according to the montmorillonite + vermiculite + chlorite + illite + kaolinite = 100% formula).

hematite, and magnetite. Iron (hydr)oxide minerals at contents below 1% can be quantified. The absolute errors between the calculated values and the known values of mineral contents below 5% were in the range of −0.49%–+0.63%. The absolute errors between the calculated values and the known values of mineral contents above 10% were in the range of −6.32%–+5.00%. The method was used to obtain the absolute contents of minerals and analyze the microstructure of iron (hydr) oxide minerals in the five natural soil clay fractions with high- or low-content iron (hydr)oxide minerals in China. The contents and compositions of minerals in the natural soil clay fractions and the degrees of Al-substitution in the (hydr)oxides obtained from the Rietveld method indicate that the order of pedogenic development of the soils is GY > WH > SD and WGS > WGL, respectively. The order of pedogenic development of the natural soils is consistent with the conclusions obtained from the magnetic properties and chemical extraction of iron (hydr)oxides. The relative amount of hematite increases and those of goethite and magnetite/maghemite decrease with the increase in pedogenesis. The goethite indicates cold and dry conditions, whereas the hematite indicates warm and wet conditions.

Acknowledgements

The authors acknowledge the support of the National Natural Science Foundation of China (Nos. 41101218 and 41330852), funding by Northwest A&F University (Z109021120), and the Western Light Project of the Chinese Academy of Sciences (K318001103).

References

Alves, M.E., Omotoso, O., 2009. Improving rietveld-based clay mineralogic quantification of oxisols using Siroquant. Soil Sci. Soc. Am. J. 73, 2191–2197.
Alves, M.E., Mascarenhas, Y.P., French, D.H., Vaz, C.P.M., 2007. Rietveld-based mineralogical quantitation of deferrified oxisol clays. Aust. J. Soil Res. 45, 224–232.
Antao, S.M., Hassan, I., Wang, J., Lee, P.L., Toby, B.H., 2008. State-of-the-art high-resolution powder X-ray diffraction (Hrpxrd) illustrated with Rietveld structure refinement of quartz, sodalite, Tremolite, and Meionite. Can. Mineral. 46, 1501–1509.
Arduino, E., Barberis, E., Ajmone Marsan, F., Zanini, E., Franchini, M., 1986. Iron oxides and clay minerals within profiles as indicators of soil age in northern Italy. Geoderma 37, 45–55.
Arocena, J.M., Sanborn, P., 1999. Mineralogy and genesis of selected soils and their implications for forest management in central and northeastern British Columbia. Can. J. Soil Sci. 79, 571–592.
Balan, E., Lazzeri, M., Morin, G., Mauri, F., 2006. First-principles study of the OH-stretching modes of gibbsite. Am. Mineral. 91, 115–119.
Banfield, J.F., Murakami, T., 1998. Atomic-resolution transmission electron microscope evidence for the mechanism by which chlorite weathers to 1: 1 semi-regular chlorite-vermiculite. Am. Mineral. 83, 348–357.
Barrón, V., Torrent, J., 2013. Iron, manganese and aluminium oxides and oxyhydroxides. In: Nieto, F., Livi, K.J.T., Oberti, R. (Eds.), Minerals at the Nanoscale. Mineralogical Society of Great Britain and Ireland, pp. 297–336.
Bish, D.L., Von Dreele, R.B., 1989. Rietveld refinement of non-hydrogen atomic positions in kaolinite. Clay Clay Miner. 37, 289–296.
Blake, R.L., Hessevick, R.E., Zoltai, T., Finger, L.W., 1966. Refinement of the hematite structure. Am. Mineral. 51, 123–129.
Brinatti, A.M., Mascarenhas, Y.P., Pereira, V.P., Partiti, C.S.d.M., Macedo, Á., 2010. Mineralogical characterization of a highly-weathered soil by the Rietveld method. Sci. Agric. 67, 454–464.
Cooperative Research Group on Chinese Soil Taxonomy (Eds.), 2001. Chinese Soil Taxonomy. Science Press, Beijing and New York.
Cornell, R.M., Schwertmann, U., 2003. The Iron Oxides: Structure, Properties, Reactions, Occurences and Uses, Second ed. Wiley-WCH, Weinheim.
Dekkers, M.J., 1997. Environmental magnetism: an introduction. Geol. Mijnb. 76, 163–182.
Dere, A.L., White, T.S., April, R.H., Brantley, S.L., 2016. Mineralogical transformations and soil development in shale across a latitudinal climosequence. Soil Sci. Soc. Am. J. 80, 623–636.
Dias, N.M.P., Gonçalves, D., Leite, W.C., Brinatti, A.M., Saab, S.C., Pires, L.F., 2013. Morphological characterization of soil clay fraction in nanometric scale. Powder Technol. 241, 36–42.
Drits, V.A., Zviagina, B.B., McCarty, D.K., Salyn, A.L., 2010. Factors responsible for crystal-chemical variations in the solid solutions from illite to aluminoceladonite and from glauconite to celadonite. Am. Mineral. 95, 348–361.
Fey, M.V., Dixon, J.B., 1981. Synthesis and properties of poorly crystalline hydrated aluminous goethites. Clay Clay Miner. 29, 91–100.
Fine, P., Singer, M.J., Verosub, K.L., 1992. Use of magnetic-susceptibilitpy measurements in assessing soil uniformity in chronosequence studies. Soil Sci. Soc. Am. J. 56, 1195–1199.
Fine, P., Singer, M.J., Verosub, K.L., Tenpas, J., 1993. New evidence for the origin of ferrimagnetic minerals in loess from China. Soil Sci. Soc. Am. J. 57, 1537–1542.
Fitzpatrick, R.W., Schwertmann, U., 1982. Al-substituted goethite - an indicator of pedogenic and other weathering environments in South Africa. Geoderma 27, 335–347.
Fontes, M.P.F., Weed, S.B., 1991. Iron oxides in selected Brazilian Oxisols: I. Mineralogy. Soil Sci. Soc. Am. J. 55, 1143–1149.
Geiss, C.E., Zanner, C.W., Banerjee, S.K., Joanna, M., 2004. Signature of magnetic enhancement in a loessic soil in Nebraska, United States of America. Earth Planet. Sci. Lett. 228, 355–367.
Gold, D.C., Bowen, L.H., B, W.S., M, B.J., 1979. Mössbauer studies of synthetic and soil-occurring aluminum-substituted goethites. Soil Sci. Soc. Am. J. 43, 802–808.
Guo, Z., Biscaye, P., Wei, L., Chen, X., Peng, S., Liu, T., 2000. Summer monsoon variations over the last 1.2 ma from the weathering of loess-soil sequences in China. Geophys. Res. Lett. 27, 1751–1754.
Gylesjö, S., Arnold, E., 2006. Clay mineralogy of a red clay–loess sequence from Lingtai, the Chinese Loess Plateau. Glob. Planet. Chang. 51, 181–194.
Hao, Q., Guo, Z., 2001. Quantitative measurements on the paleo-weathering intensity of the loess-soil sequences and implication on paleomonsoon. Sci. China Ser. D. 44, 566–576.
Hardy, R.G., Tucker, M.E., 1988. X-ray powder diffraction of sediments. In: Tucker, M.E. (Ed.), Techniques in Sedimentology. Blackwell, Oxford UK, pp. 191–228.
Hazemann, J.-L., Bérar, J.F., Manceau, A., 1991. Rietveld studies of the aluminium-iron substitution in synthetic goethite. Mater. Sci. Forum 79-82, 821–826.
Hendricks, S.B., Jefferson, M.E., 1938. Crystal structure of vermiculites and mixed vermiculite-chlorites. Am. Mineral. 23, 851–862.
Huang, C., Zhao, W., Liu, F., Tan, W., Koopal, L.K., 2011. Environmental significance of mineral weathering and pedogenesis of loess on the southernmost loess plateau, China. Geoderma 163, 219–226.
Huang, C.-Q., Zhao, W., Li, F.-Y., Tan, W.-F., Wang, M.-K., 2012. Mineralogical and pedogenetic evidence for palaeoenvironmental variations during the Holocene on the loess plateau, China. Catena 96, 49–56.
IUSS Working Group WRB, 2014. World Reference Base for Soil Resources 2014. World Soil Resources Reports No. 106. FAO, Rome.
Ji, J., Balsam, W., Chen, J., 2001. Mineralogic and climatic interpretations of the Luochuan loess section (China) based on diffuse reflectance spectrophotometry. Quat. Res. 56, 23–30.
Kunze, G.W., Dixon, J.B., 1986. Pretreatment for mineralogical analysis. In: Klute, A. (Ed.), Methods of Soil Analysis: Part 1. Physical and Mineralogical Methods, 2nd Edition. ASA, Madison, WI.
Lagoeiro, L.E., 1998. Transformation of magnetite to hematite and its influence on the dissolution of iron oxide minerals. J. Metamorph. Geol. 16, 415–423.
Lister, J.S., Bailey, S.W., 1967. Chlorite polytypism: IV. Regular two-layer structures. Am. Mineral. 52, 1614–1631.
Liu, T.S. (Ed.), 1985. Loess and the Environment. China Ocean Press, Beijing (In Chinese).

Liu, X.M., Heller, F., Liu, D.S., Xu, T.C., 1992a. Magnetic-susceptibility of chinese loess as a paleoclimatic indicator. Sci. China Ser. B. 35, 612–620.
Liu, X.M., Shaw, J., Liu, T.S., Heller, F., Yuan, B.Y., 1992b. Magnetic mineralogy of chinese loess and its significance. Geophys. J. Int. 108, 301–308.
Liu, F., Xu, F., Li, X., Wang, Y., Zeng, G., 1994. Types of crystalline Iron oxides and phosphate adsorption in variable charge soils. Pedosphere 4, 35–46.
Lutterotti, L., Scardi, P., 1990. Simultaneous structure and size–strain refinement by the Rietveld method. J. Appl. Crystallogr. 23, 246–252.
Malengreau, N., Bedidi, A., Muller, J.P., Herbillon, A.J., 1996. Spectroscopic control of iron oxide dissolution in two ferralitic soils. Eur. J. Soil Sci. 47, 13–20.
Mehra, O.P., Jackson, M.L., 1960. Iron oxide removal from soils and clays by a dithionite–citrate buffered with sodium bicarbonate. Clay Clay Miner. 7, 317–327.
Mizota, C., Longstaffe, F., 1996. Origin of cretaceous and Oligocene kaolinites from the Iwaizumi clay deposit, Iwate, northeastern Japan. Clay Clay Miner. 44, 408–416.
Nelson, D.W., Sommers, L.E., 1982. Total Carbon, Organic Carbon and Organic Matter, in: Methods of Soil Analysis. ASA and SSSA, Madison, Wisconsin USA, pp. 534–580.
O'Neill, H.S.C., Dollase, W.A., 1994. Crystal structures and cation distributions in simple spinels from powder XRD structural refinements: $MgCr_2O_4$, $ZnCr_2O_4$, Fe_3O_4 and the temperature dependence of the cation distribution in $ZnAl_2O_4$. Phys. Chem. Miner. 20, 541–555.
Pai, C.W., Wang, M.K., Wang, W.M., Houng, K.H., 1999. Smectites in iron-rich calcareous soil and black soils of Taiwan. Clay Clay Miner. 47, 389–398.
Prandel, L.V., Saab, S.C., Brinatti, A.M., Giarola, N.F.B., Leite, W.C., Cassaro, F.A.M., 2014. Mineralogical analysis of clays in hardsetting soil horizons, by X-ray fluorescence and X-ray diffraction using Rietveld method. Radiat. Phys. Chem. 95, 65–68.
Rapp, G.R., Hill, C.L. (Eds.), 2006. Geoarchaeology: The Earth-Science Approach to Archaeological Interpretation. Yale University Press.
Schulze, D.G., 1984. The influence of aluminum on iron oxides. VIII. Unit-cell dimensions of Al-substituted goethites and estimation of Al from them. Clay Clay Miner. 32, 36–44.
Schwertmann, U., 1964. Differenzierung der eisenoxide des bodens durch extraktion mit ammoniumoxalat-lösung. Z. Pflanzenernähr. Dueng. Bodenkd. 105, 194–202.
Schwertmann, U., Cornell, R.M. (Eds.), 2000. Iron Oxides in the Laboratory-Preparation and Characterization. Wiley-WCH, Weinheim, Germany.
Schwertmann, U., Kämpf, N., 1985. Properties of goethite and hematite in kaolinitic soils of southern and Central Brazil. Soil Sci. 139, 344–350.
Schwertmann, U., Taylor, R.M., 1989. Iron oxides. In: Dixon, J.B., Weed, S.B. (Eds.), Minerals in Soil Enironments, 2nd Edition. Soil Science Society of America, Madison, Wisconsin, pp. 379–438.
Schwertmann, U., Fitzpatrick, R.W., Taylor, R.M., Lewis, D.G., 1979. The influence of aluminum on iron oxides. Part II. Preparation and properties of Al-substituted hematites. Clay Clay Miner. 27, 105–112.
Schwertmann, U., Murad, E., Schulze, D., 1982. Is there holocene reddening (hematite formation) in soils of axeric temperate areas? Geoderma 27, 209–223.
Shu, J., Dearing, J.A., Morse, A.P., Yu, L., Yuan, N., 2001. Determining the sources of atmospheric particles in Shanghai, China, from magnetic and geochemical properties. Atmos. Environ. 35, 2615–2625.
Singer, A., 1980. The paleoclimatic interpretation of clay minerals in soils and weathering profiles. Earth-Sci. Rev. 15, 303–326.
Stokes, G.G., 1845. On the theories of the internal friction of fluids in motion and of the equilibrium and motion of elastic solids. T. Camb. Phil. Soc. 8, 287–319.
Torrent, J., Schwertmann, U., Schulze, D.G., 1980. Iron oxide mineralogy of some soils of two river terrace sequences in Spain. Geoderma 23, 191–208.
Torrent, J., Liu, Q.S., Barrón, V., 2010. Magnetic susceptibility changes in relation to pedogenesis in a Xeralf chronosequence in northwestern Spain. Eur. J. Soil Sci. 61, 161–173.
Viani, A., Gualtieri, A.F., Artioli, G., 2002. The nature of disorder in montmorillonite by simulation of X-ray powder patterns. Am. Mineral. 87, 966–975.
Weidler, P.G., Luster, J., Schneider, J., Sticher, H., Gehring, A.U., 1998. The Rietveld method applied to the quantitative mineralogical and chemical analysis of a ferralitic soil. Eur. J. Soil Sci. 49, 95–105.
Wilson, M.J., 1999. The origin and formation of clay minerals in soils: past, present and future perspectives. Clay Miner. 34, 7–25.
Wilson, M.J., 2004. Weathering of the primary rock-forming minerals: processes, products and rates. Clay Miner. 39, 233–266.
Wiriyakitnateekul, W., Suddhiprakarn, A., Kheoruenromne, I., Smirk, M.N., Gilkes, R.J., 2007. Iron oxides in tropical soils on various parent materials. Clay Miner. 42, 437–451.
Xiong, Y. (Ed.), 1985. Soil Colloid. Science Press, Beijing, China (In Chinese).